

Atorvastatin calcium loaded chitosan nanoparticles: *in vitro* evaluation and *in vivo* pharmacokinetic studies in rabbits

Abdul Baquee Ahmed^{1,*}, Ranjit Konwar¹, Rupa Sengupta²

¹Girijananda Chowdhury Institute of Pharmaceutical Science, Azara, Guwahati, India, ²ROFEL, Shri G.M.Bilakhia College of Pharmacy, Vapi, Gujarat, India.

In this study, we prepared atorvastatin calcium (AVST) loaded chitosan nanoparticles to improve the oral bioavailability of the drug. Nanoparticles were prepared by solvent evaporation technique and evaluated for its particle size, entrapment efficiency, zeta potential, *in vitro* release and surface morphology by scanning electron microscopy (SEM). In addition, the pharmacokinetics of AVST from the optimized formulation (FT5) was compared with marketed immediate release formulation (Atorva[®]) in rabbits. Particle size of prepared nanoparticles was ranged between 179.3 ± 7.12 to 256.8 ± 8.24 nm with a low polydispersity index (PI) value. Zeta potential study showed that the particles are stable with positive values between 13.03 ± 0.32 to 46.90 ± 0.49 mV. FT-IR studies confirmed the absence of incompatibility of AVST with excipient used in the formulations. *In vitro* release study showed that the drug release was sustained for 48 h. Results of pharmacokinetics study showed significant changes in the pharmacokinetic parameter (2.2 fold increase in AUC) of the optimized formulation as compared to marketed formulation (Atorva[®]). Thus, the developed nanoparticles evidenced the improvement of oral bioavailability of AVST in rabbit model.

Uniterms: Atorvastatin calcium/oral bioavailability/experimental study. Atorvastatin calcium/*in vitro* release. Atorvastatin calcium/pharmacokinetics. Nanoparticles/drugs bioavailability.

No presente estudo, preparamos nanopartículas de quitosana com atorvastatina cálcica (AVST) para melhorar a biodisponibilidade oral do fármaco. As nanopartículas foram preparadas pela técnica de evaporação de solvente, avaliando-se a granulometria, a eficiência de encapsulamento, o potencial zeta, a liberação *in vitro* e a morfologia da superfície, por meio da microscopia eletrônica de varredura (MEV). Além disso, a farmacocinética da formulação otimizada de AVST (FT5) foi comparada com a formulação comercial, de liberação imediata, comercializada (Atorva[®]), em coelhos. O tamanho das nanopartículas variou na faixa de 179,3 a $256,8 \pm 7,12 \pm 8,24$ nm, com baixo índice polidispersibilidade (PI). O estudo do potencial Zeta mostrou que as partículas são estáveis, com valores positivos entre $13,03 \pm 0,32$ a $46,90 \pm 0,49$ mV. Os estudos de FT-IR confirmaram a ausência de incompatibilidade de AVST com o excipiente utilizado nas formulações. O estudo de liberação *in vitro* mostrou que liberação sustentada do fármaco por 48 horas. Os resultados do estudo farmacocinético mostraram alterações significativas nos parâmetros (aumento de 2,2 vezes na ASC) da formulação otimizada em relação à comercializada (Atorva[®]). Assim, o desenvolvimento de nanopartículas evidenciou a melhora da biodisponibilidade oral de AVST em coelhos.

Uniterms: Atorvastatina cálcica/biodisponibilidade oral/estudo experimental. Atorvastatina cálcica/liberação *in vitro*. Atorvastatina cálcica/farmacocinética. Nanopartículas/biodisponibilidade de fármacos.

*Correspondence: Abdul Baquee Ahmed. Girijananda Chowdhury Institute of Pharmaceutical Science. Hathkhowapara, Azara. Guwahati-781017, India. E-mail: baquee1977@gmail.com, rupasengupta222@rediffmail.com

INTRODUCTION

Oral ingestion is the most convenient and commonly employed route of drug delivery due to its ease of administration, high patient compliance, cost effectiveness, least sterility constraints and flexibility in the design of dosage form. However, the major problem with the design of oral dosage forms lies with their poor bioavailability. The oral bioavailability depends on several factors including aqueous solubility, drug permeability, dissolution rate, first pass metabolism and susceptibility to efflux mechanisms. The most frequent causes of low bioavailability are attributed to poor solubility and low permeability (Yellela, 2010).

Nanoparticles (NP) are a type of colloidal drug delivery system comprising particles with a size range from 10 to 1000 nm in diameter. Nanoparticles may or may not exhibit size-related properties that differ significantly from those observed in fine particles or bulk materials (Buzea, Pacheco, Robbie, 2007). The uptake of nanoparticulate systems (NPSs) through the gastrointestinal tract (GIT) is today a well-known and accepted phenomenon, NPS uptake from the gut can provide an additional drug administration route; each system has its own pharmacokinetic parameters and specific drug-carrying ability. The bioactive molecule is transported into the GIT by carriers whose physicochemical characteristics must be taken into account, although the physicochemical and pharmacological characteristics of the drug remain intact (Kreuter, 1991; Hussain, Jaitely, Florence, 2001; Florence, Hussain, 2001; Nishioka, Yoshino, 2001; Hans, Lowman, 2002).

Peyer's patches are the most important structural units of the gut associated with lymphoid tissue (GALT); they are characterized by M-cells that overlie the lymphoid tissue and are specialized for endocytosis and transport into intraepithelial spaces and adjacent lymphoid tissue. Nanoparticles bind to the apical membrane of M-cells, after which they are rapidly internalized and "shuttled" to the lymphocytes. The lymphatic absorption of a drug via the GALT has an advantage over the portal blood route, because it avoids presystemic metabolism by the liver (hepatic first-pass effect) (Florence, Hussain, 2001; Hans, Lowman, 2002).

Nanoparticles were first developed for the parenteral route; more recently, they have also been studied as oral delivery vehicles. The major interest is in the lymphatic uptake of nanoparticles by Peyer's patches in the GALT (Bala, Hariharan, Kumar, 2004). Microparticles remain in Peyer's patches, while nanoparticles are disseminated systemically (Hans, Lowman, 2002). Clearly, a wide

variety of drugs can be delivered via the oral route using polymeric nanoparticulate carriers and much of the research has focused on the absorption enhancement of peptides proteins, and vaccine antigens (Delie, Blanco-Prieto, 2005).

Mucoadhesive ability can be conferred to NPSs by coating their surface with microadhesive polymers such as chitosan or Carbopol; action is more effective and prolonged, confirming the usefulness of mucoadhesive properties (Takeuchi, Yamamoto, Kawashima, 2001). Insulin entrapped in PACA nanospheres dispersed in an oily phase containing a surfactant produces prolonged hypoglycemia (Damage *et al.*, 1997b). The fate of poly (isobutylcyanoacrylate) nanocapsules carrying insulin administered to rats was monitored by fluorescence and transmission electron microscopy (TEM) and evidenced intestinal absorption through the epithelial mucosa (Pinto-Alphandary *et al.*, 2003). A luminescent polymer was used as a visible tracer to monitor the oral fate of PLGA microspheres containing insulin (Li, Jang, Jin, 2004). The therapeutic effects of another peptide, octreotide, can be improved and prolonged on incorporation into PACA nanocapsules (Damage *et al.*, 1997a).

AVST, (3R,5R)-7-[2-(4-fluorophenyl)-3-phenyl-4-(phenylcarbamoyl)-5-propan-2-ylpyrrol-1-yl]-3,5-dihydroxyheptanoic acid, calcium salt (2:1) trihydrate, is a BCS class II drug used in the treatment of hypercholesterolemia. It is insoluble in aqueous solutions at pH 4 and below. It exhibits low oral bioavailability of 14% which is ascribed to the presystemic clearance in the gastrointestinal mucosa and extensive hepatic first pass metabolism. It acts by competitive inhibition of HMG-CoA reductase, hence; it prevents the conversion of HMG-CoA to mevalonate, an early rate-limiting step in the biosynthesis of cholesterol (Lennernas, 2003).

In this study, we prepared AVST loaded chitosan nanoparticles to improve the oral bioavailability of AVST. The usefulness of AVST loaded chitosan nanoparticles was evaluated by measuring its particle size and surface morphology, loading efficiency, drug release profile, and pharmacokinetics parameters in rabbits to fully characterize the system.

MATERIAL AND METHODS

Atorvastatin calcium and amlodipine besylate were obtained as gift sample from Ozone Pharmaceutical, Guwahati, India. Chitosan and Pluronic F68 were procured from Balaji drugs, India. All other chemicals and solvents used are of analytical grade.

Drug-excipient compatibility study by FT-IR spectroscopy (Ahmed, Nath, 2014)

FT-IR spectra were recorded on a Bruker spectrophotometer (Model-220, Germany) using KBr discs in the range of 4000-450 cm^{-1} . FT-IR analysis was performed using sample of AVST with various excipients at 1:1 mass/mass ratio.

Preparation of drug loaded Chitosan nanoparticles

AVST loaded chitosan nanoparticles were prepared by the emulsion–diffusion–evaporation method (Yadav *et al.*, 2012) as per the composition shown in Table I. In brief, 10 mg of AVST and 10-50 mg of chitosan (1:1 to 1:5, drug to polymer ratio) were dissolved in 20 ml of acetone-acetic acid mixture (1:2 ratio) at room temperature for 2 h. The organic phase was then added to 50 ml of an aqueous phase containing Pluronic F68 (4% w/v) as stabilizer. The resulting primary o/w emulsion was stirred at 1000 rpm for 1 h and subsequently homogenized at 24,000 rpm for 5 min using a high-speed homogenizer (IKA T25 digital Ultra Turrax, Germany). To this emulsion, water was added with constant stirring to facilitate diffusion and finally evaporate the organic solvent. This resulted in polymer precipitation and formation of nanoparticles. Free drug and surfactant were separated by centrifuging (REMI cooling centrifuge, Vasai) the drug loaded nanoparticles at 10,000 \times g for 20 min.

Characterization of nanoparticles

Particle size and zeta potential (Patil *et al.*, 2009)

Hydrodynamic diameter and zeta potential of nanoparticles were determined using Zetasizer Nano ZS 90 dynamic light scattering equipment (Malvern Instruments Ltd. UK). Nanoparticles (~1 mg/mL) were dispersed in distilled water using sonication prior to particle size and zeta potential determinations. Mean hydrodynamic diameters were calculated based on size distribution by

weight, assuming a lognormal distribution, and the results were expressed as mean \pm S.D. of five runs. Zeta potential values were calculated from measured velocities, and results were expressed as mean \pm S.E.M. of five runs.

Encapsulation efficiency (Zhu *et al.*, 2010)

Loading of AVST in chitosan nanoparticles were determined by extracting 5 mg nanoparticles with 1 mL acetone for 6 h. From this solution 0.2 mL was diluted with phosphate buffer pH 6.8 and analyzed by UV spectrophotometer (Shimadzu UV-1800, Japan) at 264 nm against appropriate blank. Drug loading and encapsulation efficiency were calculated by using equation Eq. (1) and Eq. (2) respectively:

$$\% \text{ Drug Loading} = \frac{\text{Amount of drug in nanoparticles (mg)}}{\text{Amount of nanoparticles (mg)}} \quad \text{Eq. (1)}$$

$$\% \text{ Entrapment Efficiency} = \frac{\text{Amount of drug in nanoparticles (mg)}}{\text{Initial amount of drug (mg)}} \quad \text{Eq. (2)}$$

In vitro release (Wilson *et al.*, 2008)

Drug release from nanoparticles was determined in 0.1 N HCl and phosphate buffer pH 6.8 at 37 °C. Nanoparticle suspension (1 mg/mL, 0.5 mL) was placed in a dialysis tube (cellulose membrane, Sigma Chemical Company, USA) and immersed in 10 mL of the release buffer in a 15-mL centrifuge tube and shaken in an incubator shaker set at 100 rpm. At predetermined time intervals, 1 mL of the buffer solution was removed from the tube and analyzed for drug content by UV spectrophotometer (Shimadzu UV-1800, Japan) at 264 nm against appropriate blank.

Kinetic analysis of the release data

AVST release from nanoparticles was studied

TABLE I - Composition of AVST nanoparticles

F. No.	AVST (mg)	chitosan (mg)	Pluronic F68 (mg)	Acetone-acetic acid mixture (1:2 ratio) mL	Distilled water (mL)
F1	10	10	2	20	50
F2	10	20	2	20	50
F3	10	30	2	20	50
F4	10	40	2	20	50
F5	10	50	2	20	50

by various mathematical models described elsewhere (Ghosal; Ray, 2011). These models were applied taking into account the amount of drug released from 1 to 48 hours at different intervals as determined in release studies *in-vitro*. Various equations employed in this study were zero-order model; first order model, Higuchi square root equation and Korsmeyer–Peppas model due to their simplicity and applicability (Ghosal, *et al.*, 2012; Li, *et al.*, 2006).

The mathematical expressions for the semi-empirical models are as follows:

$$Q_t = K_0 t + C_0 \quad \text{Eq. (3)}$$

$$Q_t = K_H \sqrt{t} + C_H \quad \text{Eq. (4)}$$

$$\ln Q_t = \ln Q_0 + K_t \quad \text{Eq. (5)}$$

where Q_t is the cumulative percentage amount of drug released at time t , Q_0 is the initial amount of drug in nanoparticles, K_0 , K_H , K_t , are release rate constants, and C_0 , C_H are the respective y-intercepts in the absorbance vs. time curve. Korsmeyer–Peppas model was used specifically to explore release mechanisms and the fraction of drug release (Eq. 6) (Korsmeyer *et al.*, 1983).

$$(M_t/M_\infty) = kt^n \quad \text{Eq. (6)}$$

where k is a constant incorporating the structural and geometric characteristics of the matrix tablets, n is the release exponent, indicative of the drug release mechanism and (M_t/M_∞) represents the drug dissolved fraction at time t . To clarify the release exponent for different formulations, the log value of the percentage drug released was plotted against log time according to Eq. (7).

$$\text{Log } (M_t/M_\infty) = \text{log } k + n \text{ log } t \quad \text{Eq. (7)}$$

During the Korsmeyer–Peppas model fitting, we obtained the value of the release exponent n , which conveys information on whether the release mechanism is Fickian, non-Fickian or case II transport mechanism. In this context, $n=0.5$ indicates Fickian release (diffusion controlled release) and $n=1$ indicates a purely relaxation-controlled delivery, which is referred to as case II transport. When the value of n is intermediate, it indicates an anomalous behaviour (non-Fickian kinetics corresponding to coupled diffusion/polymer relaxation). A value of $n > 1$ indicates super case II kinetics.

Scanning electron microscopy (SEM) of nanoparticles

The shape and surface characteristics of the nanoparticles were observed by scanning electron

microscopy (SEM). The nanoparticle sample was thinly sprinkled onto a metal stub and vacuum coated with a thin layer of gold in an argon atmosphere. The SEM photomicrographs of the coated particles were obtained at 15 kV using a ZEISS, Germany, scanning electron microscope (Thangaraja, Savitha, Jegatheesan, 2010).

Pharmacokinetics studies

The study was carried out to compare the pharmacokinetics parameters of AVST from a prepared nano formulation (F5) to a conventional commercially available immediate release tablet formulation (Atorva®, 10) following oral administration of doses 2.4 mg/kg in two groups of animals (five in each group). The study was approved by Institutional Animal Ethics Committee of Girijananda Chowdhury Institute of Pharmaceutical Science; vide no. 1372/c/10/CPCSEA.

The animals used for study were male albino rabbits weighing about 1.5–2 kg, obtained from Animal House of Girijananda Chowdhury Institute of Pharmaceutical Science, Guwahati, India. The animals were kept under standard laboratory conditions at a temperature of 25 ± 2 °C and relative humidity ($55 \pm 5\%$). The animals were divided into two groups as Group-I and Group-II. Each rabbit of Group- I was given marketed formulation dose (2.4 mg/kg) according to their weight using oral feeding needle. Same dose of nanoparticle suspension was administered to Group-II animals. About 0.5 mL of blood samples were collected from orbital sinus at interval of 0.5, 1, 1.5, 2, 2.5, 3, 4, 6, 8, 10, 12 and 24 hr into microfuse tube containing 15 μ L Sodium Citrate (3.3% w/v) solution for each sample and centrifuged at 5000 rpm for 15 min at 4 °C to separate plasma. The separated plasma samples were frozen at -20 °C till analysis.

Plasma sample analysis

Then 200 μ L of each plasma sample was taken into a 5 mL centrifuge tube and 50 μ L of amlodipine besylate (AMDP) solution (50 μ g/mL) was added as an internal standard (IS) and the mixtures were vortexed for 30 s. After that, 2 mL acetonitrile was added into the mixture, vortexed for additional 2 min and centrifuged at 10,000 rpm for 10 min. The supernatant was transferred into a glass centrifuge tube and evaporated to dryness at 45 °C under a stream of nitrogen. The residue was reconstituted with 200 μ L of reconstitution solvent (mobile phase). The samples were filtered through 0.45 μ m membrane filter using syringe filter. An aliquot of 20 μ L of the sample was injected onto the HPLC column for analysis.

The HPLC system consisted of a Dual pump, (Model M515, Waters corp., USA) and UV-Visible detector (Model M2489, Waters corp., USA) set at a wavelength of 264 nm. The samples were chromatographed on a reverse phase NOVA-PAK HR C18 column (4 μm , 150 \times 3.9 mm, Ireland). The mobile phase consisting of acetonitrile and 0.05 M ammonium acetate solution in the ratio of 45:55 (v/v) with an apparent pH 6.09 was filtered through a 0.45 μm membrane filter and degassed under vacuum before use. It was pumped at a flow rate of 1.5 mL/min for the run time of 10 min under these experimental conditions with an injection volume of 20 μL of the sample solution (Rheodyne Injector, Model 7725i) (Waters corp. USA). The amount of drug present in 200 μL of plasma [(quantity obtained from regression equation/200) \times 1000] was calculated.

Extraction efficiency and validation of bio-analytical methods

For recovery of drug from plasma different organic extraction solvents (ethyl acetate, acetonitrile and methanol) were tried in the experiment and acetonitrile was proved to be the most efficient in extracting AVST from rabbit plasma and had a small variation in extraction recoveries over the concentration range. Spiked plasma sample was prepared in triplicate at single concentration of 30 $\mu\text{g/mL}$ of AVST and 50 $\mu\text{g/mL}$ of IS, and assayed as described above. The extraction efficiency of AVST was determined by comparing the peak areas measured after analysis of spiked plasma sample with those found after direct injection of non-biological (unextracted) samples into the chromatographic system at the same concentration levels.

The bio-analytical method was validated for specificity, recovery, linearity and precision. The specificity of the method was determined by comparing the chromatograms obtained from the solution of AVST and IS with those from blank plasma. Linearity of the calibration curve was determined by taking nine different concentrations (0.2 -50 $\mu\text{g/mL}$) of AVST with fixed concentration of IS (50 $\mu\text{g/mL}$) in blank plasma. The calibration curve was plotted between the ratio of peak areas of AVST to IS and concentration of AVST. Both repeatability (within a day precision) and reproducibility (between days precision) were determined. Four quality control samples were subjected for the study. Five injections of each of the specified quality control samples were injected for analysis within the same day for repeatability, and over a period of 5 days for reproducibility. The relative standard deviations (RSD) and percent coefficient of variation (%CV) were calculated

and used to predict the precision of the method.

Determination of pharmacokinetics parameters

The pharmacokinetic parameters were determined from the data of plasma drug concentration at different time points by using MS-Excel 2003 software according to the procedure described elsewhere (Jambhekar, Breen, 2009; Bourne, 2001).

Data and statistical analysis

Data are represented as mean \pm SD (n=5). Statistical comparisons were made using one-way analysis of variance (ANOVA). A value of $p < 0.05$ was considered statistically significant. All data processing was performed using the SPSS[®] statistical software program (SPSS[®] 14, Microsoft, USA).

RESULTS AND DISCUSSION

FT-IR analysis of drug–excipients mixture

FT-IR spectroscopy study was carried out to test the compatibility of AVST with chitosan and Pluronic F68 used as polymer and stabilizer in the formulation. FT-IR spectra of AVST showed presence of characteristics band at 3362 cm^{-1} for (-OH), 3236 cm^{-1} for (-NH), 2971 cm^{-1} for (-CH₃), 2824 cm^{-1} for (-CH aromatic), 1649 cm^{-1} for (C=O), 1578 cm^{-1} for (C-N), and 1432 cm^{-1} for (C-C) functional groups. All these characteristics bands were also retained in 1:1 physical mixture of AVST-chitosan and AVST-Pluronic F68 showed in Figure 1. The results clearly revealed the incompatibility of drug with the excipients used in the formulation.

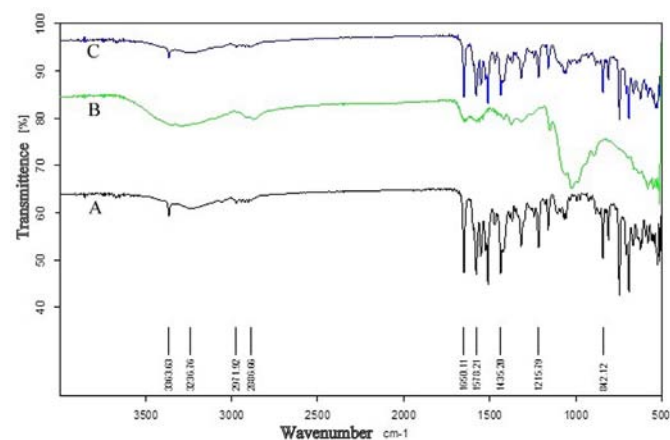


FIGURE 1 - FT-IR spectra of AVST (A), chitosan (B) and 1:1 physical mixture of AVST and chitosan (C).

Physico-chemical characterization of AVST loaded nanoparticles

The Physico-chemical characteristics of AVST-loaded chitosan nanoparticles were summarized in Table II. The result showed the high yield of nanoparticle i.e. 66.66 ± 0.73 to $85.71 \pm 0.68\%$. The average loading of AVST in nanoparticles were about $4 \pm 1.1\%$, $9 \pm 1.0\%$, $13 \pm 0.92\%$, $15 \pm 0.93\%$, $16 \pm 0.80\%$ and encapsulation efficiency of $8.02 \pm 2.2\%$, $25.2 \pm 2.8\%$, $48.10 \pm 3.4\%$, $72.02 \pm 4.5\%$, $96.01 \pm 4.8\%$ in formulation F1, F2, F3, F4, F5 respectively. The average loading and encapsulation efficiency in the formulations were found to be increase with increase in polymer concentration used in the formulations. A maximum of $16 \pm 0.80\%$ drug loading and $96.01 \pm 4.8\%$ entrapment efficiency was observed at 1:5, drug to polymer ratio in formulation F5, the change in drug loading may be due to the poor aqueous solubility and high binding capacity of drug on polymer surface in organic solvent used in the nanoparticle formulation.

The result showed the average size of prepared nanoparticles varied from 179.3 ± 7.12 to 256.8 ± 8.24 nm with a polydispersity index (PI) in the range of 0.461 ± 0.002 to 0.252 ± 0.004 as shown in Table II. Size of nanoparticle was increased with increase in polymer concentration. Nevertheless, the PI was found to be always lower than 0.5, which is considered as an evidence of a homogeneous nanoparticle formulation. On the other hand, in all the AVST-loaded nanoparticles formulations had zeta potential value of 13.03 ± 0.32 to 46.9 ± 0.49 mV. The net positive surface charge of all formulations may be due to the use cationic polyelectrolyte (chitosan) and the addition of Pluronic F68 in the formulation aids to reduce aggregation of nanoparticles may results the stability of the formulations. The average droplet of the selected formulation F5 by dynamic light scattering determination was 46.9 ± 0.49 mV (Figure 2).

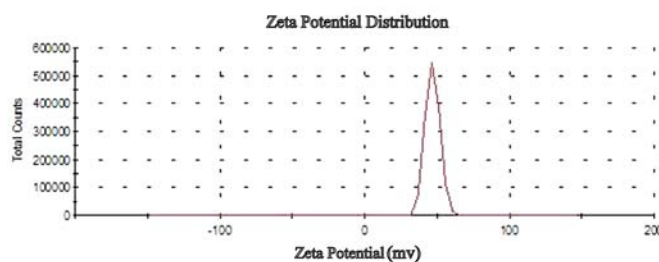


FIGURE 2-AVERAGE zeta potential of the formulation F5 containing 1:5 ratio of drug to polymer measured by dynamic light scattering method.

In vitro drug release studies

In vitro release profiles of AVST loaded chitosan nanoparticles in 0.1N Hydrochloric acid and Phosphate buffer pH 6.8 are shown in Figure 3 and Figure 4 respectively. Sustained release of drug was observed from the formulations in 0.1N Hydrochloric acid and Phosphate buffer pH 6.8 for duration 48 hours. It was found that as the concentration of polymer increased in the formulations drug release was sustained for longer period, which may be

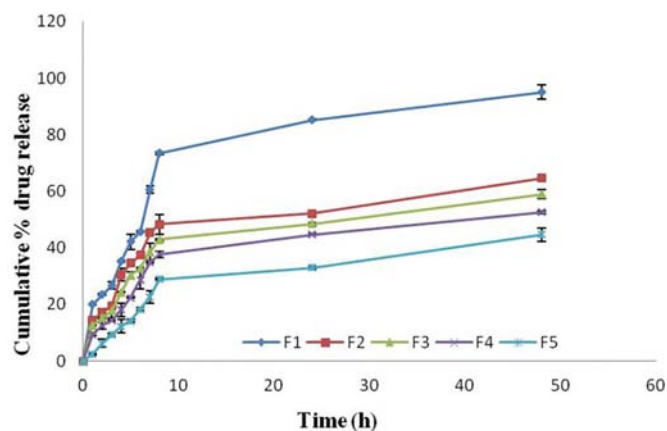


FIGURE 3 - In vitro drug release profile for different formulations in 0.1 N HCl.

TABLE II - Physico-chemical characterization of AVST-loaded chitosan nanoparticles

F. No.	D:Pol ratio	Size(nm)	ZetaPotential (mV)	Yield (%)	EE (%)	PI
F1	1:1	179.3 ± 7.12	13.03 ± 0.32	66.66 ± 0.73	8.02 ± 2.2	0.461 ± 0.002
F2	1:2	201.2 ± 8.23	19.77 ± 0.45	70.01 ± 0.70	25.20 ± 2.8	0.318 ± 0.012
F3	1:3	227.8 ± 5.19	23.10 ± 0.58	74.02 ± 0.68	48.10 ± 3.4	0.326 ± 0.015
F4	1:4	238.9 ± 9.21	29.16 ± 0.43	80.10 ± 0.75	72.02 ± 4.5	0.283 ± 0.008
F5	1:5	256.8 ± 8.24	46.90 ± 0.49	85.71 ± 0.68	96.01 ± 4.8	0.252 ± 0.004

Data expressed as the mean \pm SD (n=3). EE: Encapsulation efficiency PI: Polydispersity Index D: Pol (Drug: Polymer).

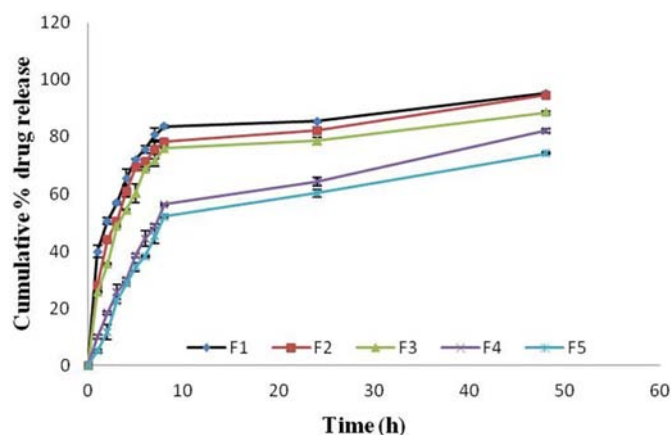


FIGURE 4 - *In vitro* drug release profile for different formulations in Phosphate buffer pH 6.8.

due to the hydration ability of chitosan, which on coming in contact with dissolution media leads to the formation of gelatinous mass and act as retardant material for the drug to diffuse out. Thus a prolonged release of drug is attained and at the end of 48 hours, the cumulative % drug release from formulations F1, F2, F3, F4, F5 was 95.04 ± 0.48 , 64.6 ± 0.52 , 58.94 ± 0.56 , 52.54 ± 0.52 , 44.62 ± 0.32 in 0.1N Hydrochloric acid and 95.24 ± 0.38 , 94.6 ± 0.44 , 88.54 ± 0.54 , 82.1 ± 0.54 , 74.12 ± 0.28 in Phosphate buffer pH 6.8 respectively. Thus F5 formulation contained higher percentage of polymer (1:5, Drug: polymer ratio) was able to sustain the release of drug for long period of time (more than 48 h) compared to other formulations in 0.1 N hydrochloric acid medium.

Kinetics and mechanism of drug release

The *in vitro* drug release data was fitted into appropriate equations, the correlation coefficient (R) and the release rate constant was determined from the slope of the respective equations for all formulations (Table III). Among all the formulations F5 found to be best fitted in Higuchi kinetics with R_H value of 0.9149, followed by zero order ($R_O=0.8763$) and first order ($R_F=0.7400$) kinetics.

This explains that drug release from the nanoparticle formulations followed primarily diffusion controlled release mechanism. Further, to confirm the drug release mechanism from the nanoparticle formulations the *in vitro* drug release data at various time points were fitted into the Korsmeyer-Peppas equation. The correlation coefficient (R_p values) of 0.9571, 0.9636, 0.9591, 0.9651 and 0.9828 for the formulations F1, F2, F3, F4 and F5 respectively which showed good linearity between log cumulative amount of drug release versus log time, and the highest linearity was observed with F5, where drug to polymer concentration was maximum (1:5). The release exponents (n_p values) were found to be 0.7950, 0.8165, 0.7239, 0.7456 and 0.8766 for the formulations F1, F2, F3, F4 and F5 respectively. The obtained n_p values of all the formulations were greater than 0.5 and less than 1. Hence, it is revealed that the mechanism of drug release was a non-Fickian or anomalous diffusion.

Surface morphology

Particle images obtained by SEM from F5 samples, as shown in Figure 5, indicated that produced nanoparticles were spherical in shape with smooth surface and the size of particles varied from 212.3 nm to 230.9 nm. No agglomeration and uniformly distribution of the particles confirmed the stability of formulation. Magnification of a single particle showed the internal cage like structure where the drug molecules are dispersed uniformly throughout the polymer matrix. The drug appeared as white spots on the surface. It was observed that when a high energy electron beam were passed to scan the particles in SEM, the polymer burns out leaving the drug particles viewed as a cage like structure.

Extraction efficiency and bio-analytical methods

The recovery of drug was found to be $91.25\% \pm 3.03$, $82.37\% \pm 2.07$ and 77.28 ± 1.72 (w/w) in acetonitrile, ethyl

TABLE III - Comparative release kinetics parameter of all the batches of nanoparticles

F. No.	Release kinetic parameter							
	Zero order		First order		Higuchi		Korsmeyer and Peppas	
	R_0	K_0	R_F	K_F	R_H	K_H	R_p	n_p
F1	0.8659	1.68	0.7257	0.019	0.8679	14.470	0.9571	0.7950
F2	0.8603	1.04	0.7302	0.020	0.8346	9.193	0.9636	0.8165
F3	0.8646	0.9821	0.7285	0.018	0.8710	7.942	0.9591	0.7239
F4	0.8662	0.9247	0.7852	0.016	0.8684	8.5322	0.9651	0.7456
F5	0.8763	0.8455	0.7400	0.022	0.9149	6.933	0.9828	0.8766

acetate and methanol respectively at all three concentration levels, which confirmed the extraction efficiency of the solvents. Among the solvents, acetonitrile showed maximum amount of drug recovery. Hence, acetonitrile

was selected as the extracting solvent. The recovery of IS was also found to be maximum in acetonitrile which was $96.23\% \pm 2.2$ (w/w).

Under the described conditions of the bio-analytical methods, the retention time of AVST and AMDP was found 3.0 and 2.2 min respectively (Figure 6). Absence of the interfering peaks near the retention time of the AVST as well as IS indicating the specificity of the method. The chromatographic responses (ratio of peak area of AVST to IS versus AVST concentration) were found to be linear over an analytical range of 0.2–50 $\mu\text{g/mL}$ with regression coefficient value of 0.9977, which showed reproducibility. The relative standard deviation (RSD) and percent coefficient of variation (%CV) of intra-day assay of the drug was ranged from 0.0098 to 0.0326 and 0.98 to 3.26%; for the inter-day assay was from 0.0049 to 0.0297 and 0.49 to 2.97% respectively (Table IV). The low RSD and % CV indicate the precision of the method.

Pharmacokinetics parameters

The comparison of the different pharmacokinetic parameters was done by using a one-way analysis of variance (ANOVA). A value of $p < 0.05$ was considered statistically significant. The pharmacokinetics parameters were derived from plasma drug concentrations versus time profile of all the subjects and the results are shown in Table V and Figure 7. From the pharmacokinetic study, it can be revealed that the optimised nanoparticle formulation, F5 showed better C_{max} , T_{max} and AUC than the marketed formulation (Atorva[®]) of drug. It was found that the C_{max} in plasma for optimised nanoparticle formulation (219.78 $\mu\text{g/mL}$) represents greater improvement than the marketed formulations (103.3 $\mu\text{g/mL}$). It was also observed that $\text{AUC}_{0-48\text{h}}$ of optimised nanoparticle formulation was 2618.98 $\mu\text{g}\cdot\text{hr/mL}$ and thus the difference were highly significant ($p < 0.05$) as compared to $\text{AUC}_{0-48\text{h}}$ of marketed tablet suspension (Table IV) formulation. The t_{max} of optimised nanoparticle formulation was

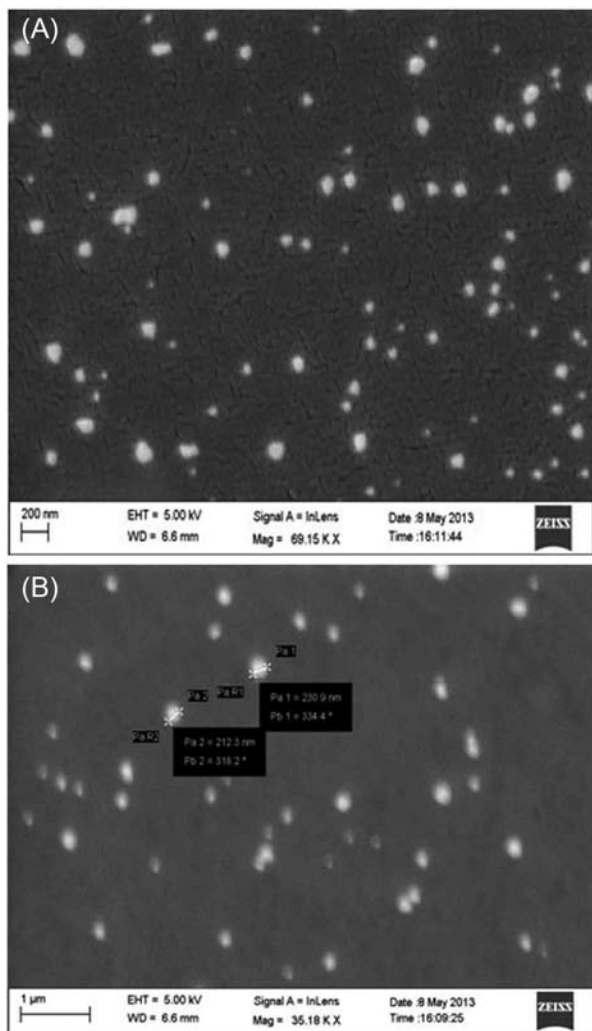


FIGURE 5 - SEM image of particles from F5 formulation (A) Nanoparticles in spherical shape with smooth surface. (B) Magnification of a single particle showed the internal cage like structure of size 212.3 to 238.9 nm.

TABLE IV - Precision and accuracy of method for the estimation of AVST in rabbit plasma

Concentration ($\mu\text{g/mL}$)	Intra-day precision			Inter-day precision		
	Mean \pm SD (n = 5) ($\mu\text{g/mL}$)	RSD	%CV	Mean \pm SD (n = 5) ($\mu\text{g/mL}$)	RSD	%CV
0.2	0.1988+0.0065	0.0326	3.26	0.1982+0.0059	0.0297	2.97
10	10.116+0.2060	0.0203	2.03	10.04+0.0894	0.0089	0.89
30	29.974+0.2962	0.0098	0.98	29.992+0.1392	0.0049	0.49
50	49.962+0.8064	0.0161	1.61	50.252+0.6157	0.0122	1.22

SD-Standard deviation, RSD-Relative Standard Deviation, CV-Coefficient of Variation

TABLE V – Pharmacokinetic parameters

Parameters	Units	Marketed formulation(Atorva®) Mean ± SD (n = 5)	Optimised formulation, F5 Mean ± SD (n = 5)
C _{max}	µg/mL	103.3 ± 1.22	219.78 ± 2.54
T _{max}	Hrs	2 ± 0.24	2 ± 0.08
AUC _{0-48h}	µg-hr/mL	1232.84 ± 2.66	2618.98 ± 2.98

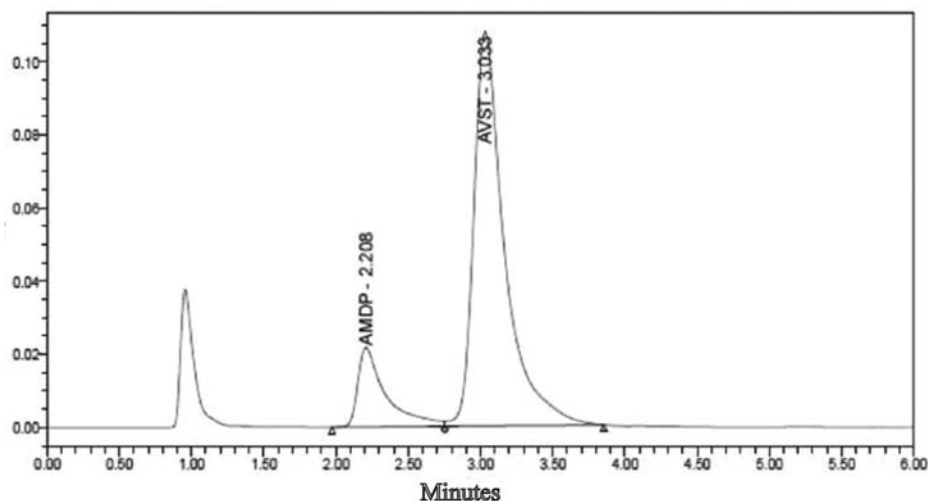


FIGURE 6 - HPLC chromatogram of AVST and internal standard (AMDP) in rabbit plasma.

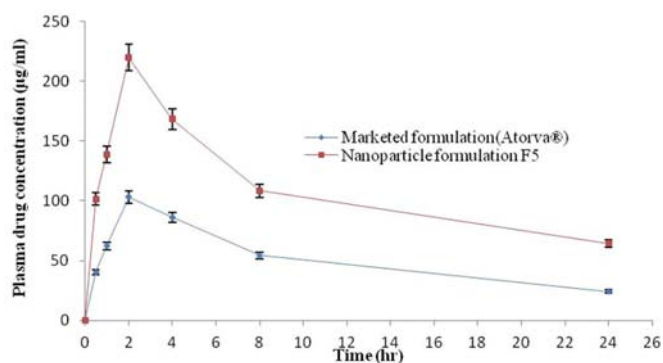


FIGURE 7 - Plasma concentration profiles of optimized formulation (F5) and marketed formulation (Atorva®) after oral administration in rabbits (mean ± SD, n = 5).

found to be similar when compared to t_{max} of marketed tablet suspension. The difference in C_{max} of optimised nanoparticle formulation was very significant ($p < 0.05$) when compared with the marketed tablet suspension. It was also observed that AUC_{0-48h} of optimised nanoparticle formulation was nearly 2.2 fold increase in the AUC for the nanoparticles as opposed to the pure drug (Atorva®). Furthermore, this result suggested the improvement of oral absorption of AVST in nanoparticle formulation, which may be due to the changes in gastrointestinal membrane

permeability of the drug and the inhibition of an apically polarized efflux system.

CONCLUSION

In conclusion stable nanoparticles with positive zeta potential value between 13.03 ± 0.32 to 46.90 ± 0.49 mV and particle size range between 179.3 ± 7.12 to 256.8 ± 8.24 nm of calcium atorvastatin was prepared successfully using solvent evaporation techniques. Nanoparticle size depends primarily on the excess of polymer added into the system and *in vitro* release study revealed the sustained release of drug for 48h. Results of pharmacokinetics study showed a significant difference in the pharmacokinetics parameter (2.2 fold increase in AUC) of the optimized formulation as compared to marketed formulation (Atorva®). Thus, the developed nanoparticles evidenced the improvement of oral bioavailability of calcium atorvastatin in rabbit model.

ACKNOWLEDGEMENT

The authors would like to thank Ozone Pharmaceutical, Guwahati, India for supplying Atorvastatin calcium and amlodipine besylate as gift sample.

REFERENCES

- AHMED, A.B.; NATH, L.K. Drug-excipients compatibility studies of nicorandil in controlled release floating tablet. *Int. J. Pharm. Pharm. Sci.*, v.6, n.2, p.468-475, 2014.
- BALA, I.; HARIHARAN, S.; KUMAR, R. PLGA nanoparticles in drug delivery: the state of the art. *Crit. Rev. Ther. Drug Carrier Syst.*, v.21, n.5, p.387-422, 2004.
- BOURNE, D.W. Pharmacokinetics. In: BANKER, G.S., RHODES, C.T. (Eds.). *Modern pharmaceuticals*. 4. ed. New York: Marcel Dekker, 2001.
- BUZEA, C.; PACHECO, I.; ROBBIE, K. Nanomaterials and nanoparticles: sources and toxicity. *Biointerphases*, v.2, n.4, p.MR17-MR71, 2007.
- DAMGÉ, C.; VONDERSCHER, J.; MARBACH, P.; PINGET, M. Poly(alkyl cyanoacrylate) nanocapsules as a delivery system in the rat for octreotide, a long-acting somatostatin analogue. *J Pharm Pharmacol.*, v.49, n.10, p.949-954, 1997a.
- DAMGE, C.; VRANKX, H.; BALSCHMIT, P.; COUVREUR, P. Poly(alkylcyanoacrylate) nanospheres for oral administration of insulin. *J Pharm Sci.*, v.86, n.12, p.1403-1409, 1997b.
- DELIE, F.; BLANCO-PRIETO, M.J. Polymeric particulates to improve oral bioavailability of peptide drugs. *Molecules*, v.10, p.65-80, 2005.
- FLORENCE, A.T.; HUSSAIN, N. Transcytosis of nanoparticle and dendrimer systems: evolving vistas. *Adv. Drug Deliver. Rev.*, v.50, p.S69-S89, 2001.
- GHOSAL, K.; RAY, S.D. Alginate/hydrophobic HPMC (60M) particulate systems: new matrix for site-specific and controlled drug delivery. *Braz. J. Pharm. Sci.*, v.47, n.4, p.833-844, 2011.
- GHOSAL, K.; CHANDRA, A.; RAJABALAYA, R.; CHAKRABORTY, S.; NANDA, A. Mathematical modeling of drug release profiles for modified hydrophobic HPMC based gels. *Pharmazie*, v.67, n.2, p.147-155, 2012.
- HANS, M.L.; LOWMAN, A.M. Biodegradable nanoparticles for drug delivery and targeting. *Curr. Opin. Solid St. Materials Sci.*, v.6, n.4, p.319-323, 2002.
- HUSSAIN, N.; JAITLEY, B.; FLORENCE, A.T. Recent advances in understanding the uptake of microparticulates across the gastrointestinal lymphatics. *Adv. Drug Deliver Rev.*, v.50, n.1-2, p.107-142, 2001.
- JAMBHEKAR, S.S.; BREEN, P.J. *Extravascular route of drug administration in basic pharmacokinetics*. London: Pharmaceutical Press, 2009. p.106-126.
- KORSMEYER, R.W.; GURNY, R.; DOELKER, E.; BURI, P.; PEPPAS, N.A. Mechanism of solute release from porous hydrophilic polymers. *Int. J. Pharm.*, v.15, n.1, p.25-35, 1983.
- KREUTER, J. Peroral administration of nanoparticles. *Adv. Drug Deliver Rev.*, v.7, n.1, p.71-86, 1991.
- LENNERNAS, H. Clinical pharmacokinetics of Atorvastatin. *Clin. Pharmacokinet.*, v.42, n.13, p.1141-1160, 2003.
- LI, S.; SHEN, Y.; LI, W.; HAO, X.A. Common profile for polymer-based controlled release and its logical interpretation to general release process. *J. Pharm. Pharm. Sci.*, v.9, n.2, p.238-244, 2006.
- LI, Y.; JANG, H.L.; JIN, J.E. Bioadhesive fluorescent microspheres as visible carriers for local delivery of drugs. II: uptake of insulin-loaded PCEFB/PLGA microspheres by the gastrointestinal tract. *Drug Deliv.*, v.11, n.6, p.335-340, 2004.
- NISHIOKA, Y.; YOSHINO, H. Lymphatic targeting with nanoparticulate systems. *Adv. Drug Deliver Rev.*, v.47, n.1, p.55-64, 2001.
- PATIL, Y.; SADHUKHAT; MAL., PANYAM, J. Nanoparticle-mediated simultaneous and targeted delivery of paclitaxel and tariquidar overcomes tumor drug resistance. *J. Control. Release*, v.136, n.1, p.21-29, 2009.
- PINTO-ALPHANDARY, H.; ABOUBAKAR, M.; JAILLARD, D.; COUVREUR, P.; VAUTHIER, C. Visualization of insulin loaded nanocapsules: in vitro and in vivo studies after oral administration to rats. *Pharm. Res.*, v.20, n.7, p.1071-1084, 2003.
- TAKEUCHI, H.; YAMAMOTO, H.; KAWASHIMA, Y. Mucoadhesive nanoparticulate systems for peptide drug delivery. *AAAdv. Drug Deliver Rev.*, v.47, n.1, p.39-54, 2001.

- THANGARAJA, A.; SAVITHA, V.; JEGATHEESAN, K. Preparation and Characterisation of Polyethylene glycol coated silica nanoparticles for drug delivery application. *IJNA*, v.4, n.1, p.31-38, 2010.
- WILSON, B.; SAMANTA, MK.; SANTHI, K.; KUMAR, KPS.; PARAMAKRISHNAN, N.; SURESH, B. Targeted delivery of tacrine into the brain with polysorbate 80 coated poly (n-butylcyanoacrylate) nanoparticles. *Eur. J. Pharm. Biopharm.*, v.70, n.1, p.75-84, 2008.
- YADAV, H.K.S.; NAGAVARMA, B.V.N.; AYAZ, A.; VASUDHA, L.S.; SHIVAKUMAR, H.G. Different techniques for preparation of polymeric nanoparticles- a review. *Asian J. Pharm. Clin. Res.*, v.5, n.3, p.16-23, 2012.
- YELLELA, S.R.K. Pharmaceutical Technologies for enhancing oral bioavailability of poorly soluble drugs. *J. Bioequiv. Availab.*, v.2, n.2, p.28-36, 2010.
- ZHU, Z.; LI, Y.; LI, X.; LI, R.; JIA, Z.; LIU, B.; GUO, W.; WU, W.; JIANG, X. Paclitaxel loaded poly (n-vinylpyrrolidone)-b-poly(ϵ -caprolactone) nanoparticles: Preparation and antitumor activity *in vivo*. *J. Control. Release*, v.142, n.3, p.438-446, 2010.

Received for publication on 11th July 2014

Accepted for publication on 09th December 2014

